

UNCLASSIFIED

AD NUMBER

AD093841

CLASSIFICATION CHANGES

TO: unclassified

FROM: confidential

LIMITATION CHANGES

TO:  
Approved for public release, distribution unlimited

FROM:  
Distribution authorized to U.S. Gov't. agencies and their contractors; Administrative/Operational Use; 17 MAY 1956. Other requests shall be referred to National Aeronautics and Space Administration, Washington, DC.

AUTHORITY

NASA TR SERVER WEBSITE; NASA TR SERVER WEBSITE

THIS PAGE IS UNCLASSIFIED

**CONFIDENTIAL**

**A  
D** **93841**

**Armed Services Technical Information Agency**

Reproduced by

**DOCUMENT SERVICE CENTER**

**KNOTT BUILDING, DAYTON, 2, OHIO**

This document is the property of the United States Government. It is furnished for the duration of the contract and shall be returned when no longer required, or upon recall by ASTIA to the following address: Armed Services Technical Information Agency, Document Service Center, Knott Building, Dayton 2, Ohio.

**NOTICE: WHEN GOVERNMENT OR OTHER DRAWINGS, SPECIFICATIONS OR OTHER DATA ARE USED FOR ANY PURPOSE OTHER THAN IN CONNECTION WITH A DEFINITELY RELATED GOVERNMENT PROCUREMENT OPERATION, THE U. S. GOVERNMENT THEREBY INCURS NO RESPONSIBILITY, NOR ANY OBLIGATION WHATSOEVER; AND THE FACT THAT THE GOVERNMENT MAY HAVE FORMULATED, FURNISHED, OR IN ANY WAY SUPPLIED THE SAID DRAWINGS, SPECIFICATIONS, OR OTHER DATA IS NOT TO BE REGARDED BY IMPLICATION OR OTHERWISE AS IN ANY MANNER LICENSING THE HOLDER OR ANY OTHER PERSON OR CORPORATION, OR CONVEYING ANY RIGHTS OR PERMISSION TO MANUFACTURE, USE OR SELL ANY PATENTED INVENTION THAT MAY IN ANY WAY BE RELATED THERETO.**

**CONFIDENTIAL**

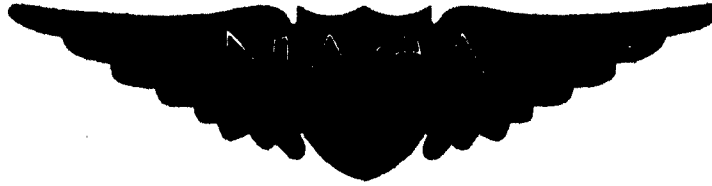
**NOTICE: THIS DOCUMENT CONTAINS INFORMATION AFFECTING THE  
NATIONAL DEFENSE OF THE UNITED STATES WITHIN THE MEANING  
OF THE ESPIONAGE LAWS, TITLE 18, U.S.C., SECTIONS 793 and 794.  
THE TRANSMISSION OR THE REVELATION OF ITS CONTENTS IN  
ANY MANNER TO AN UNAUTHORIZED PERSON IS PROHIBITED BY LAW.**

**CONFIDENTIAL**

NACA RM A56B27a

AD No. 9384

ASTIA FILE COPY



# RESEARCH MEMORANDUM

A METHOD OF REDUCING HEAT TRANSFER TO BLUNT BODIES

BY AIR INJECTION

By Jackson R. Stalder and Mamoru Inouye

Ames Aeronautical Laboratory  
Moffett Field, Calif.

# FC

CLASSIFIED DOCUMENT

This material contains information affecting the National Defense of the United States within the meaning of the espionage laws, Title 18, U.S.C., Secs. 793 and 794, the transmission or revelation of which in any manner to an unauthorized person is prohibited by law.

## NATIONAL ADVISORY COMMITTEE FOR AERONAUTICS

WASHINGTON

May 17, 1956

**CONFIDENTIAL**

MAY 24 1956

56AA

24760

## NATIONAL ADVISORY COMMITTEE FOR AERONAUTICS

RESEARCH MEMORANDUM

## A METHOD OF REDUCING HEAT TRANSFER TO BLUNT BODIES

## BY AIR INJECTION

By Jackson R. Stalder and Mamoru Inouye

## SUMMARY

Investigations were made of the effect of air injection at the stagnation point on the heat-transfer characteristics of a hemisphere in a supersonic stream. The tests were conducted at a Mach number of 2.7 and over a Reynolds number range from  $2.7 \times 10^5$  to  $6.5 \times 10^5$  based on the hemisphere diameter.

Air injection directly into the stream at a rate equivalent to 0.0070 of the weight flow of air swept out by the projected area of the hemisphere was found to double the heat transfer from the hemisphere. The injected air was swept back against the hemisphere where it disturbed the boundary layer and acted similarly to a flow-separation spike.

On the other hand, air injection tangent to the surface near the stagnation point at a rate equivalent to 0.0075 of the weight flow of air swept out by the projected area of the hemisphere nearly halved the convective heat-transfer rate and reduced the recovery factor by 6 percent.

## INTRODUCTION

A number of analytical and experimental investigations, including the tests of Rubesin, Pappas, and Okuno (ref. 1), have shown that fluid injection through a porous surface is an effective means of reducing convective heat transfer. The injected fluid provides an insulating layer between the surface and the boundary layer; that is, in effect, the boundary layer is thickened. However, the poor strength characteristics of porous materials are a deterrent to the use of this method because of the resultant structural problems. An improvement from a structural standpoint is fluid injection through a small number of openings. This method, as shown by Eckert and Livingood (ref. 2), is not so effective as transpiration through a porous surface but is still a means of reducing convective heat transfer. Simplifying the method of fluid injection

CONFIDENTIAL

further, Wieghardt (ref. 3) has studied the use of air injection through a single slot in a flat plate to obtain a warm air film for de-icing.

In the present investigation, interest is focused on blunt bodies because for flight at high supersonic speeds, the excessive heat transfer, in conjunction with the inability to conduct heat away rapidly, rules out the use of sharp leading edges or noses. Although the previously mentioned investigations were concerned with fluid injection from flat plates, it seems reasonable to assume that similar reductions in convective heat transfer would be realized for blunt bodies.

Therefore, this investigation was undertaken to devise a means of reducing the convective heat transfer to a blunt body by injecting air through a single opening. The particular configuration considered was a 1-inch-diameter hemisphere, which was tested in the Ames 6-inch heat-transfer wind tunnel at a Mach number of 2.7 and over a Reynolds number range from  $2.7 \times 10^5$  to  $6.5 \times 10^5$  based on hemisphere diameter.

#### NOTATION

- A projected frontal area of hemisphere,  $\text{ft}^2$
- d model diameter, ft
- F injection parameter,  $\frac{w}{\rho_{\infty} V_{\infty} A}$ , dimensionless
- h average heat-transfer coefficient,  $\text{BTU}/\text{sec ft}^2 \text{ } ^{\circ}\text{F}$
- k thermal conductivity,  $\text{BTU}/(\text{sec ft}^2 \text{ } ^{\circ}\text{F}/\text{ft})$
- $N_{\text{Nu}}$  Nusselt number,  $\frac{hd}{k_{\infty}}$ , dimensionless
- q convection heat-transfer rate,  $\text{BTU}/\text{sec}$
- R Reynolds number,  $\frac{\rho_{\infty} V_{\infty} d}{\mu_{\infty}}$ , dimensionless
- S surface area of hemisphere,  $\text{ft}^2$
- T temperature,  $^{\circ}\text{R}$
- V velocity,  $\text{ft}/\text{sec}$
- w injection air weight flow rate,  $\text{lb}/\text{sec}$
- $\eta_r$  temperature recovery factor,  $\frac{T_r - T_{\infty}}{T_t - T_{\infty}}$ , dimensionless

CONFIDENTIAL

- $\rho$  density, lb/cu ft  
 $\mu$  viscosity, lb sec/ft<sup>2</sup>

#### Subscripts

- n hemisphere  
r adiabatic recovery conditions  
t stagnation conditions  
 $\infty$  free-stream conditions

### TEST EQUIPMENT AND PROCEDURE

#### Models

The 1-inch-diameter hemisphere-cylinder designed for air injection directly into the stream at the stagnation point, as illustrated in figure 1(a), was essentially the same model employed by Stalder and Nielsen (ref. 4) to investigate the effect of a spike on heat transfer from a hemisphere. A 0.070-inch-diameter hole was drilled through the stagnation point of the copper hemisphere, and tubing was attached to provide for air injection. The model was heated with a small electric heater inserted in the hemisphere, and a second electric heater was wrapped around the injection air line outside the tunnel to preheat the injection air when necessary. Iron-constantan thermocouples were installed to measure the model and injection air temperatures and to obtain the temperature gradients necessary for the calculation of conduction losses. The locations of these thermocouples are indicated in figure 1(a).

The hemisphere-cylinder designed for air injection tangent to the surface, as illustrated in figure 1(b), had the same over-all dimensions and shape as the previous model. A 1/4-inch-diameter stainless-steel cap, which was threaded into a spider pressed into the hemisphere, was used to direct the injection air tangent to the surface near the stagnation point. The forward segment of the model was blunted so that with the cap in position, the over-all shape of the model was a hemisphere. The average clearance between the outer tip of the cap and the main body was 0.034 inch. The model was heated electrically as before, and copper-constantan thermocouples, as indicated in figure 1(b), were used to measure the model temperatures.

### Test Procedure

All of the tests were conducted at steady-state temperature conditions at a Mach number of 2.7 and a stagnation temperature of 120° F in the Ames 6-inch heat-transfer wind tunnel, which is described in detail in reference 5. The stagnation pressure was varied from 20 to 50 pounds per square inch absolute to obtain a Reynolds number range from  $2.7 \times 10^5$  to  $6.5 \times 10^5$  based on the hemisphere diameter. The air injection rate was varied from 0 to 0.0150 of the weight flow of air swept out by the projected area of the hemisphere. (Dry air from the tunnel make-up air supply was used for the injection air.)

For a given set of tunnel conditions, the desired air injection rate was measured with a rotameter. For each air injection rate, the electrical input to the model heater was varied in steps by use of two variable transformers in series. The average hemisphere temperature varied from a minimum of 70° F to a maximum of 170° F. The local hemisphere temperatures differed from the average by less than 2° F in the high temperature range and by less than 1/2° F in the low temperature range. The injection air was preheated in order to match its temperature upon exit from the hemisphere to within 1/2° F of the average hemisphere temperature. After steady-state conditions had been reached for each model heating rate, the thermocouple and electrical input readings and tunnel conditions were recorded.

### DATA REDUCTION

The free-stream conditions were calculated, with the assumption of isentropic flow, from the measured stagnation temperature and pressure and free-stream static pressure.

The heat input to the model heater was corrected for losses due to conduction into the support, convection to the injection air, resistance in the heater leads, radiation, and conduction along the injection air tube. The last three losses totaled less than 5 percent of the heat input. For the model with air injection directly into the stream, the proximity of the model heater to the injection air tube resulted in a considerable heat loss to the injection air. Excepting the instances of low heat input to the model, the total losses were at the maximum one-half of the total heat input. The resulting heat-transfer data are estimated to be accurate to within ±25 percent with air injection and ±7.5 percent with no air injection. For the model with air injection tangent to the surface, the heater was moved away from the injection air tube, and the major heat loss was due to conduction to the stainless-steel support shell. Again, excepting the instances of low heat input,

the total losses were at the maximum one fourth of the total heat input. For this model, the heat-transfer data are estimated to be accurate to within  $\pm 7.5$  percent for all air injection rates.

The equation for heat transfer from the hemisphere to the stream is as follows:

$$q = hST_t \left( \frac{T_n}{T_t} - \frac{T_r}{T_t} \right)$$

For a given set of tunnel conditions and air injection rate, the heat transfer by convection from the hemisphere was plotted as a function of the average hemisphere temperature, normalized by division by the stagnation temperature. (The inclusion of the stagnation temperature adjusted the data for the effect of small changes in the stagnation temperature during a heating run.) The data, when plotted in this fashion, directly yielded the average heat-transfer coefficient and the average recovery temperature since the slope of the curve was  $hST_t$  and the zero intercept occurred at  $T_r/T_t$ . The fact that the slope was constant indicated that the heat-transfer coefficient was independent of the model temperature for the temperature range of the tests.

The air injection rate was expressed in terms of the parameter  $F$ , which is defined as the ratio of the air injection rate to the weight flow of air swept out by the projected area of the hemisphere.

$$F = \frac{w}{\rho_\infty V_\infty A}$$

For various values of the air injection parameter  $F$ , the heat-transfer coefficient expressed in terms of a Nusselt number, and the recovery temperature expressed in terms of a recovery factor were plotted as functions of the Reynolds number based on the hemisphere diameter. All dimensionless quantities were based on free-stream properties.

## RESULTS AND DISCUSSION

### Air Injection Directly Into Stream

The effects of air injection directly into the stream on the flow around the hemisphere are illustrated in the shadowgraphs of figure 2. With a small amount ( $F = 0.0035$ ) of air injection, there was no change in the bow wave configuration as shown by a comparison between figures 2(a) and 2(b), but an examination of the negatives showed a small turbulent region at the stagnation point. With air injection of  $F = 0.0070$ , there was a marked change in the flow around the hemisphere as shown in figure 2(c). Sufficient air was injected to cause a rounded conical

CONFIDENTIAL

protuberance on the bow wave, followed by a violently turbulent region enveloping the hemisphere. Other shadowgraphs taken seconds apart showed small changes in the shape of the protuberance. However, in general, the flow disturbances appeared similar to those resulting from the presence of a flow-separation spike (ref. 4).

The results of the present tests, expressed in terms of average Nusselt number and recovery factor on the hemisphere with air injection directly into the stream, are shown in figures 3 and 4 as functions of the free-stream Reynolds number based on the hemisphere diameter. In addition, the results of Stalder and Nielsen (ref. 4) for spiked and unspiked hemispheres are included. For the case of no air injection, there is good agreement with the results for the unspiked hemisphere. With an air injection rate of  $F = 0.0035$ , the disturbance of the boundary layer had no effect on the recovery factor but it increased the Nusselt number 10 percent.

Air injection of  $F = 0.0070$  had an effect on the average Nusselt number and recovery factor similar to that of a flow-separation spike. The average Nusselt number on the hemisphere was doubled, and the lower static temperature rise through a near conical shock, rather than a normal shock, resulted in a slightly lower recovery factor. The similarity of effects can be explained by the fact that the forepart of the hemisphere was immersed in a highly turbulent region for both flow conditions. For the case of air injection, the injection air was blown into the stream as a column of air that simulated a spike and then was swept back against the hemisphere where it disturbed the boundary layer. For the case of the spiked hemisphere, the boundary layer on the spike separated and impinged on the hemisphere to produce similar effects.

#### Air Injection Tangent to Surface

The preceding results indicated that another method of air injection was required. Rather than injecting the air such that it directly opposed the free stream, it appeared possible that injecting the air tangent to the surface might bring about the desired thickening of the boundary layer and reduction of heat transfer. Shadowgraphs of the flow around the hemisphere with a cap to direct the injection air tangent to the surface are shown in figure 5. Up to an injection rate of  $F = 0.0075$  there was no marked change in the flow pattern. The shape of the bow wave was the same as with a hemisphere with no injection, and no violently turbulent regions existed. For the maximum air injection rate of  $F = 0.0150$ , disturbances were visible in the injection air flow between the cap and the main body of the model.

The average Nusselt number and recovery factor on the hemisphere with air injection tangent to the surface are shown in figures 3 and 4

together with the previous results. The agreement of the results obtained without any air injection with the previous findings indicated that the effect of the stainless-steel cap on the total heat transfer from the hemisphere was negligible.

Despite the absence of any visible effects in the shadowgraphs for an air injection rate of  $F = 0.0037$ , the recovery factor decreased 3 percent, and the heat transfer from the hemisphere was reduced to 75 percent of the zero injection value. For an air injection rate of  $F = 0.0075$ , there was still no visible effect of injection, but the recovery factor decreased 6 percent, and the heat transfer was reduced to 60 percent of the zero injection value. This latter result is in contrast to the previous doubling of heat transfer with approximately the same rate of air injection directly into the stream. Doubling the air injection rate to  $F = 0.0150$  resulted in only a small reduction of heat transfer to 54 percent of the zero injection value.

For constant values of the injection parameter  $F$ , the variation of Nusselt number with Reynolds number in figure 3 is in the form of parallel lines with slopes approximately equal to  $1/2$ . This shows that  $\frac{N_{Nu}}{\sqrt{R}}$  is approximately constant for a fixed value of  $F$ . The effect of air injection tangent to the surface is merely to reduce the value of the constant. If  $N_{Nu}$  and  $(N_{Nu})_{F=0}$  are determined for the same Reynolds number, the ratio  $\frac{N_{Nu}}{(N_{Nu})_{F=0}}$  is a function only of  $F$ . Such a plot is presented in figure 6. The upward concavity of the curve shows that the reduction in heat transfer per unit air injection rate diminishes with increased injection. When  $F$  exceeds about 0.0075, the benefits of increased injection are small.

The reduction in the effectiveness of air injection as shown in figure 6 appears, in part, to be a phenomenon inherent in air injection. In addition, at the higher air injection rates, disturbances in the injection air flow become more prominent and may also tend to reduce the effectiveness. For example, in figure 5(c) for an air injection rate of  $F = 0.0150$ , there appear disturbances in the injection air flow between the lower edge of the cap and the main body of the model. The Mach number of the injection air flow for  $F = 0.0150$  was estimated to be 0.4. Local accelerations due to sharp turns in the flow or turbulence might have been responsible for the disturbances.

The present tests were conducted with air injection into the boundary layer at the hemisphere temperature and with the injection air exit area constant. Greater reductions in hemisphere temperature could be obtained by injecting a refrigerated gas or a liquid to take advantage of cooling due to evaporation. Further tests are necessary to determine the optimum injection air exit area and configuration for a given injection rate.

Also, since the effect of injection at large distances from the slot probably diminishes due to mixing, further tests are necessary to determine the optimum slot spacing for a given application.

#### CONCLUSIONS

Tests were conducted on a hemisphere at a Mach number of 2.7 and over a Reynolds number range from  $2.7 \times 10^5$  to  $6.5 \times 10^5$  based on the hemisphere diameter. The results with small amounts of air injection near the stagnation point led to the following conclusions:

1. Air injection directly into the stream at a rate equivalent to 0.0070 of the weight flow of air swept out by the projected area of the hemisphere doubles the convective heat transfer from the hemisphere.
2. Air injection tangent to the surface at a rate equivalent to 0.0075 of the weight flow of air swept out by the projected area of the hemisphere nearly halves the convective heat transfer from the hemisphere and reduces by 6 percent the temperature recovery factor.
3. For the latter case of tangential injection through a fixed slot area, the reduction in heat transfer from the hemisphere, per unit air injection rate, diminishes with increased injection. In particular, doubling the air injection rate from  $F = 0.0075$  to  $F = 0.0150$  reduced slightly the convective heat transfer from 60 to 54 percent of the zero injection value.

Ames Aeronautical Laboratory  
National Advisory Committee for Aeronautics  
Moffett Field, Calif., Feb. 27, 1956

#### REFERENCES

1. Rubesin, Morris W., Pappas, Constantine C., and Okuno, Arthur F.: The Effect of Fluid Injection on the Compressible Turbulent Boundary Layer - Preliminary Tests on Transpiration Cooling of a Flat Plate at  $M = 2.7$  With Air as the Injected Gas. NACA RM A55I19, 1955.
2. Eckert, E. R. G., and Livingood, John N. B.: Comparison of Effectiveness of Convection-, Transpiration-, and Film-Cooling Methods With Air as Coolant. NACA TN 3010, 1953.

CONFIDENTIAL

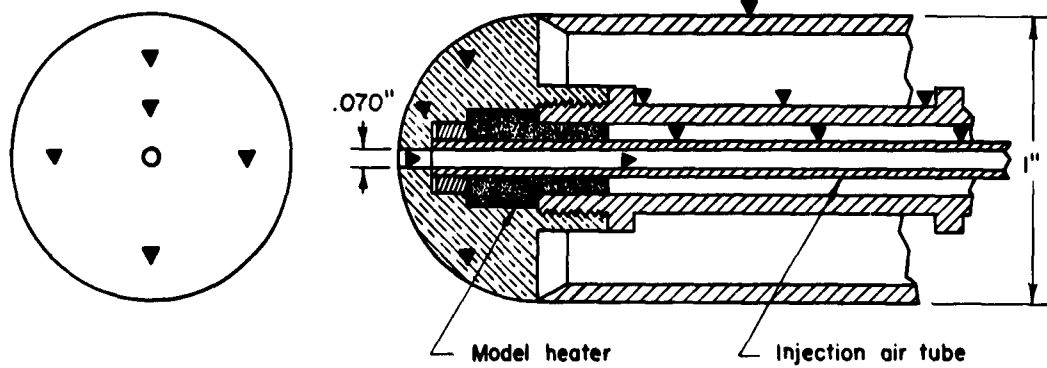
3. Wieghardt, K.: Hot-Air Discharge for De-Icing. AAF Trans. No. F-TS-919-RE, Air Mat. Com., Wright Field, Dec. 1946.
4. Stalder, Jackson R., and Nielsen, Helmer L.: Heat Transfer From a Hemisphere-Cylinder Equipped With Flow-Separation Spikes. NACA TN 3287, 1954.
5. Stalder, Jackson R., Rubesin, Morris W., and Tendeland, Thorval: A Determination of the Laminar-, Transitional-, and Turbulent-Boundary-Layer Temperature-Recovery Factors on a Flat Plate in Supersonic Flow. NACA TN 2077, 1950.

10

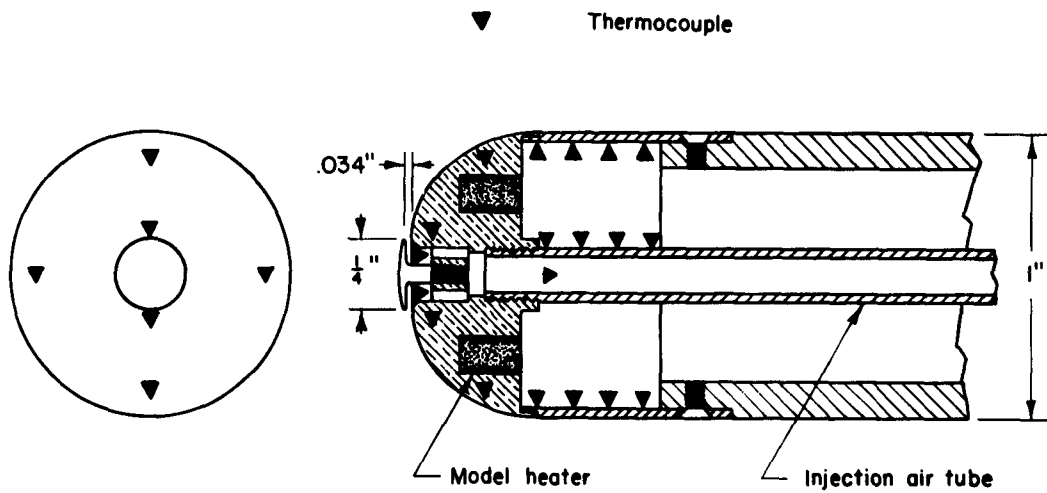
CONFIDENTIAL

NACA RM A56B27a

CONFIDENTIAL



(a) Hemisphere - cylinder with air injection directly into stream.



(b) Hemisphere - cylinder with air injection tangent to surface.

Figure 1.- Sketch of models tested.

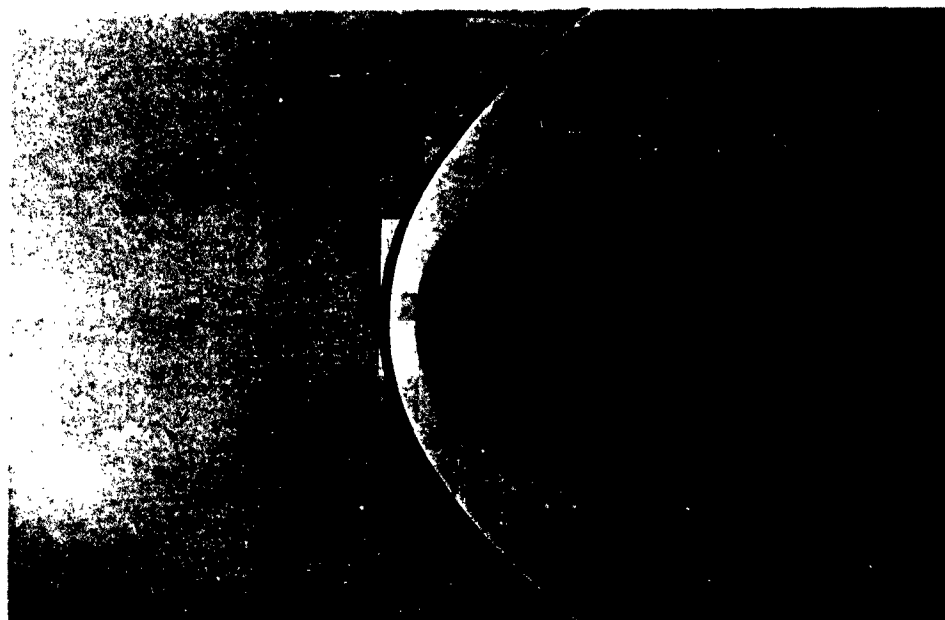
(a)  $F = 0$ (b)  $F = 0.0035$ 

Figure 2.- Shadowgraphs with air injection directly into stream;  
 $R = 6.5 \times 10^5$ .

CONFIDENTIAL



(c)  $F = 0.0070$

Figure 2.- Concluded

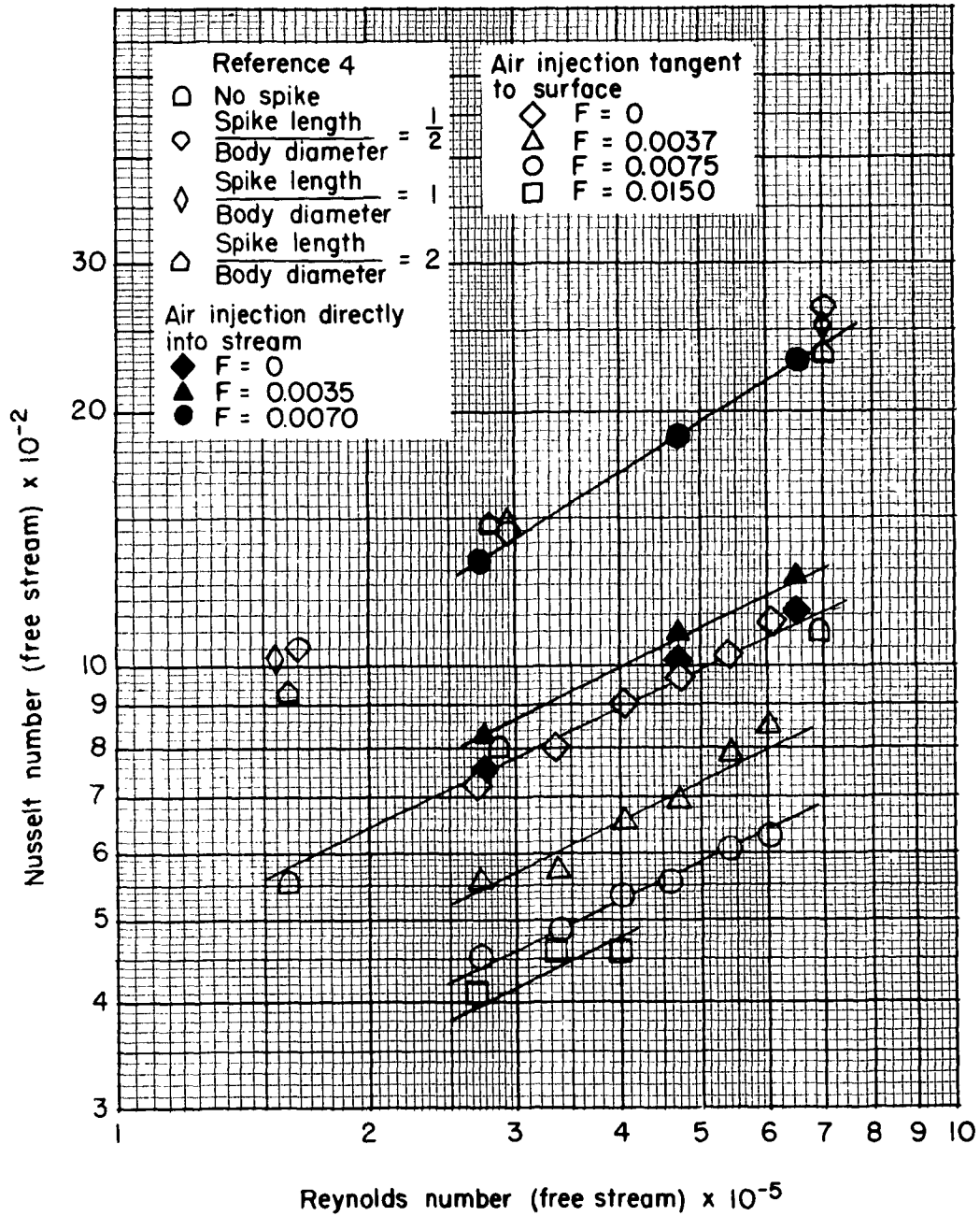


Figure 3.- Average heat transfer from hemispherical nose with, and without, air injection.

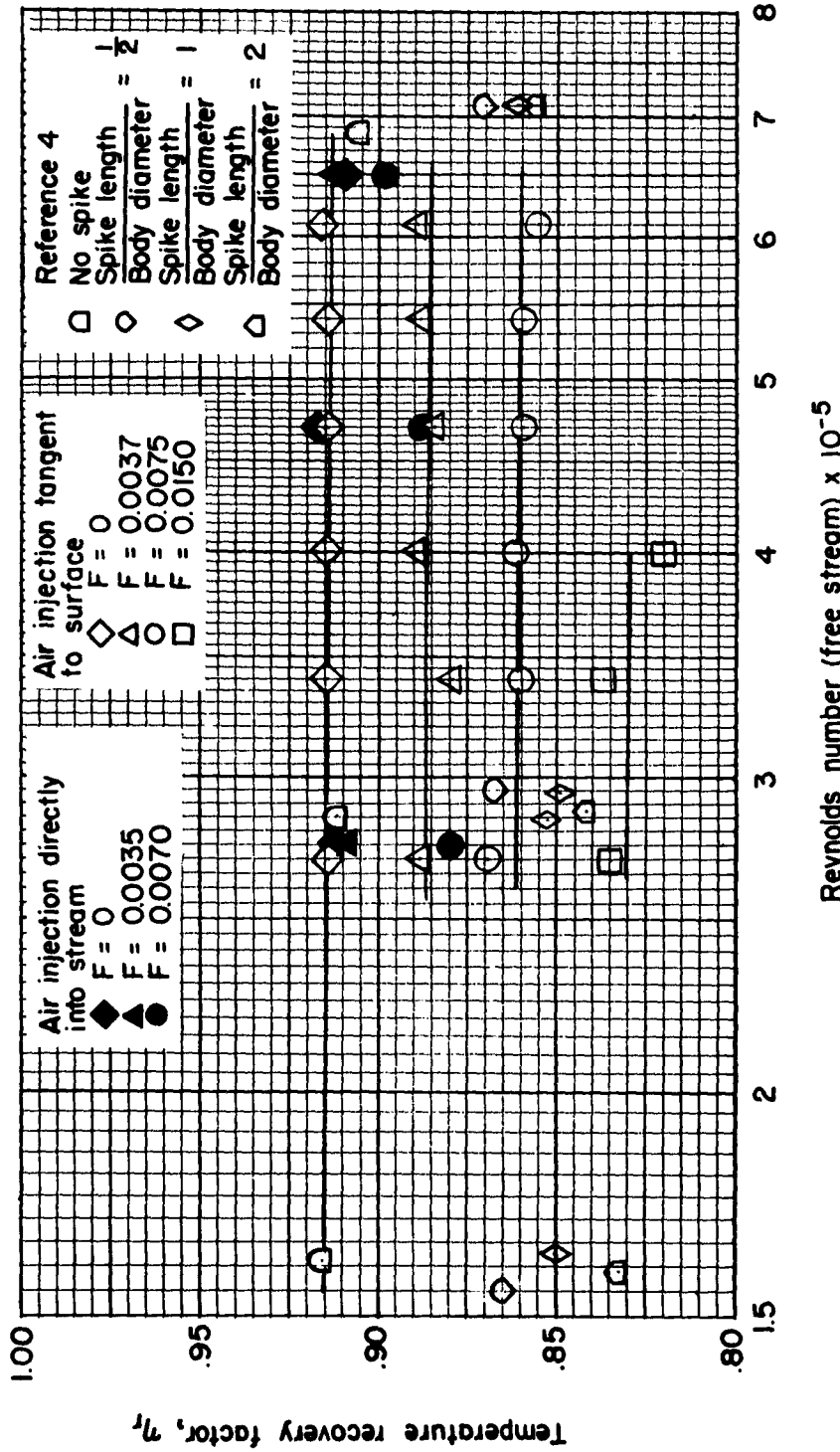


Figure 4.- Average temperature recovery factor for hemispherical nose with, and without, air injection.

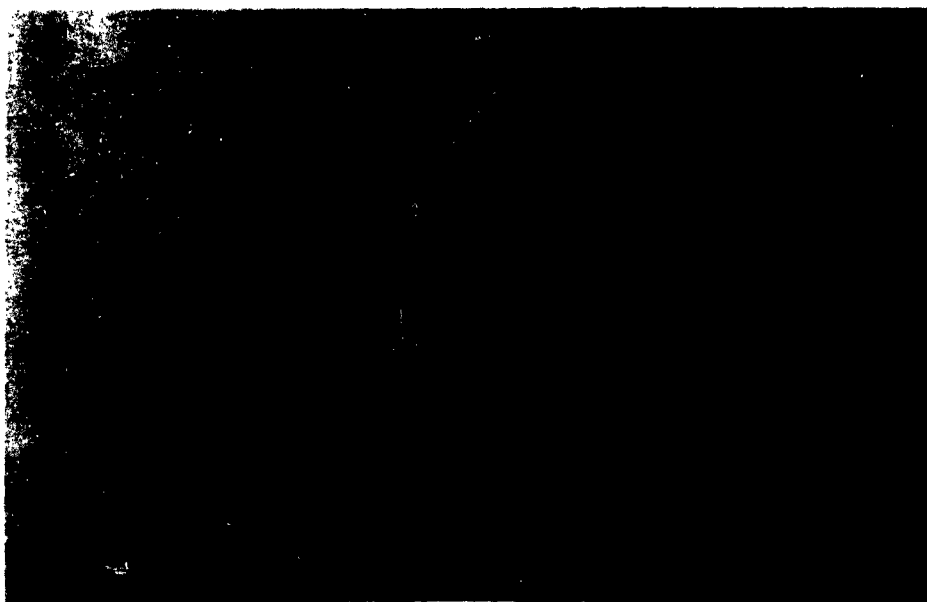
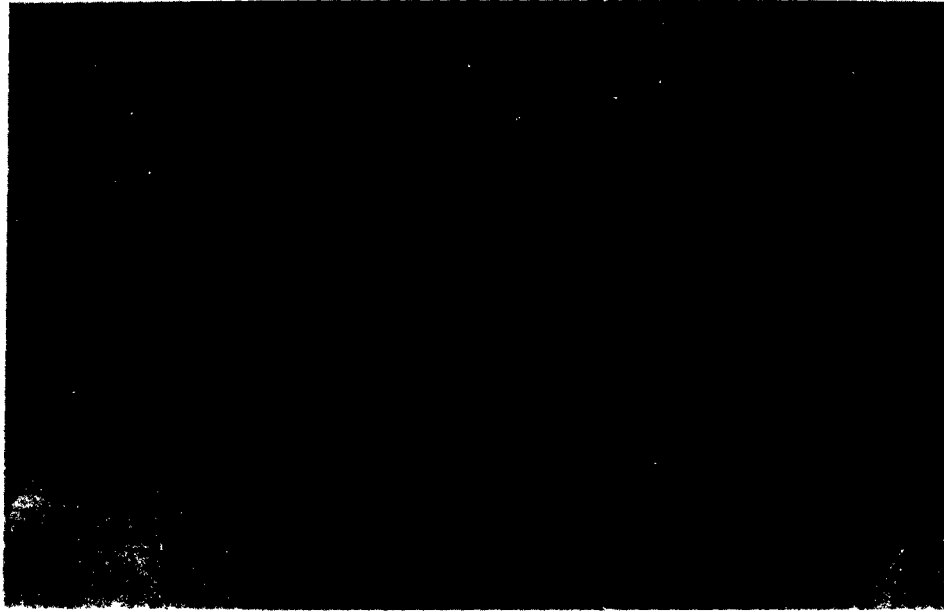
(a)  $F = 0$ (b)  $F = 0.0075$ 

Figure 5.- Shadowgraphs with air injection tangent to surface,  
 $R = 4.0 \times 10^5$ .



(c)  $F = 0.0150$

Figure 5.- Concluded

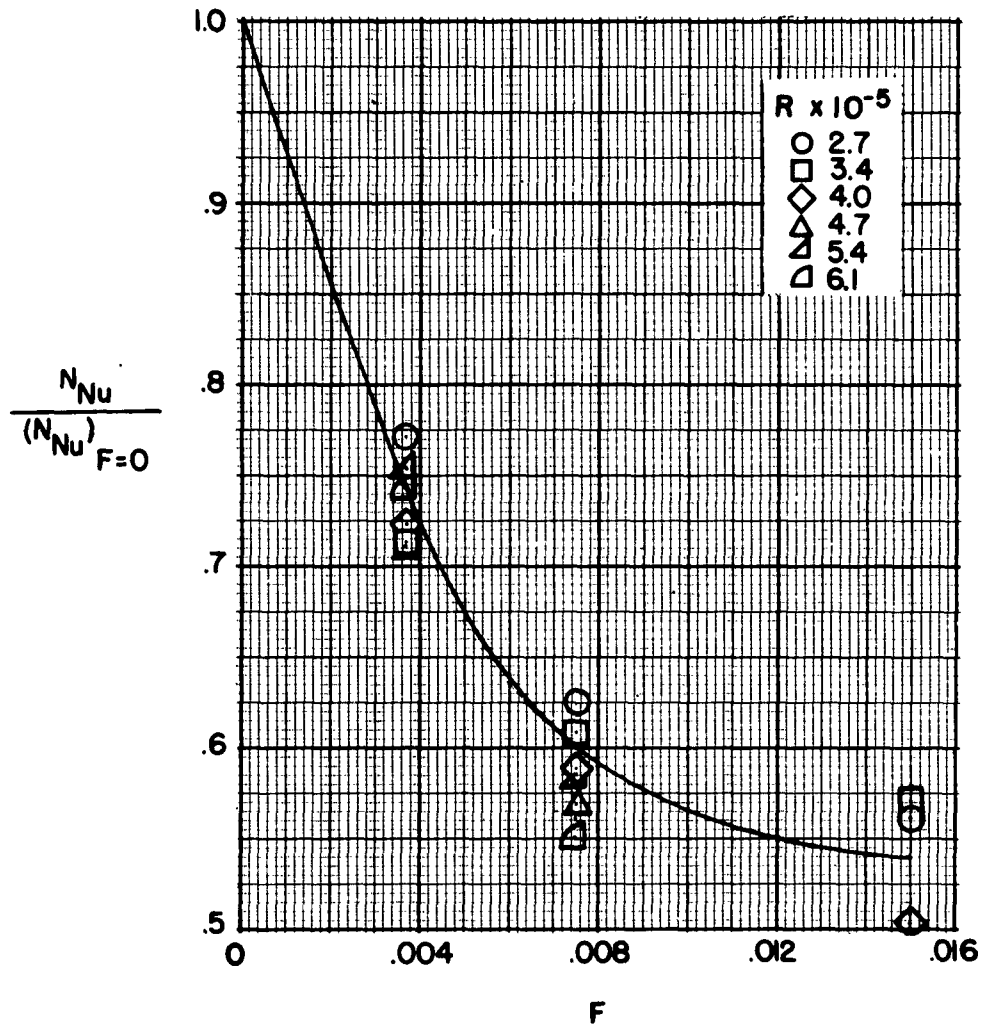


Figure 6.- Variation of ratio of average Nusselt number with air injection rate;  $N_{Nu}$  and  $(N_{Nu})_{F=0}$  calculated for same Reynolds number.